Available online at www.sciencedirect.com
SCIENCE DIRECT®
Medical Laser Application 20 (2005) 193–200
Medical Laser Application
www.elsevier.de/mla

Nanoprocessing of subcellular targets using femtosecond laser pulses

Iva Maxwell, Samuel Chung, Eric Mazur*

Department of Physics and Division of Engineering and Applied Sciences, Harvard University, 17 Oxford Street, Cambridge, MA 02138, USA

Received 2 June 2005; accepted 12 July 2005

Abstract

In this paper we review the work done in our laboratory on femtosecond laser dissection within single cells and living organisms. Precise dissection of biological material with ultrashort laser pulses requires a clear understanding of the pulse-energy dependence of the onset and extent of plasma-mediated ablation (i.e., the removal of material). We carried out a systematic study of the energy dependence of the plasma-mediated ablation of fluorescently-labeled subcellular structures in the cytoskeleton and in nuclei of fixed endothelial cells using femtosecond, near-infrared laser pulses focused through a high-numerical aperture objective lens (1.4 NA). We performed laser nanosurgery in live cells, where we ablated a single mitochondria and severed cytoskeletal filaments without compromising the cell membrane or the cell's viability. We also cut dendrites in living *C. elegans* without affecting the neighboring neurons. This nanoprocessing technique enables non-invasive manipulation of the structural machinery of cells and tissues down to several hundred nanometer resolution.

Keywords: Femtosecond laser; Nanosurgery

Introduction

Femtosecond laser pulses have two primary applications in biology: first, imaging cellular structures in microscopy [1–3] and second, micromanipulating and dissecting nanoscale structures in living cells and other biological materials [4–9]. The laser-pulse energy differentiates the two applications. When femtosecond laser pulses are focused by high numerical aperture objectives (NA > 1), the laser radiation is confined to a very small focal volume, creating photon densities high enough to induce multiphoton absorption at the laser focus, even in normally transparent materials. In imaging applications, the laser-pulse energy is kept low enough to limit the multiphoton absorption to fluorescent dyes or autofluorescent structures in the sample, and no structural damage occurs. If the energy per pulse increases above a certain threshold, a combination of multiphoton absorption and avalanche ionization generates very high concentrations of free electrons in the focal volume, resulting in plasma-mediated ablation of material in the focal region [10].

There are two key advantages in using Ti:sapphire femtosecond lasers for imaging and bulk ablation of biological samples. First, the laser wavelength is centered in the near-infrared around 800 nm where melanin, hemoglobin, and water have low absorption so the laser light can penetrate the tissue (Fig. 1, [2]). The interaction between the femtosecond laser pulses and

*Corresponding author. Fax: +1 617 496 4654.
E-mail address: mazur@physics.harvard.edu (E. Mazur).

1615-1615/$ - see front matter © 2005 Elsevier GmbH. All rights reserved.
doi:10.1016/j.mla.2005.07.005

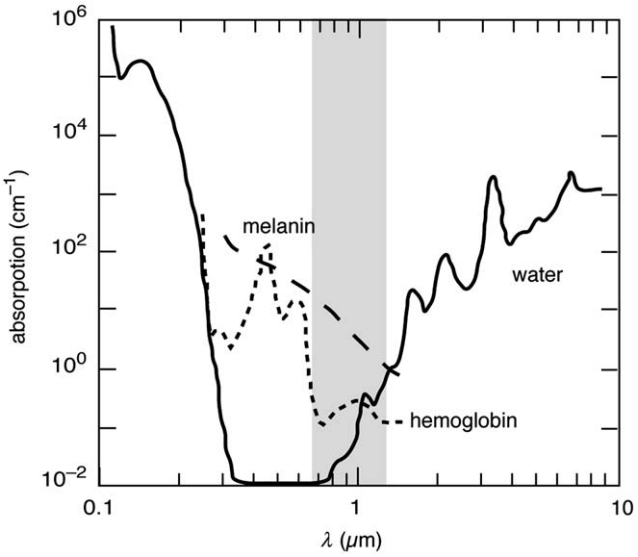

Fig. 1. Absorption spectra of the major absorbers found in tissue. There are no efficient one-photon absorbers in the cells and tissues in the near-infrared spectra, making them nearly transparent in this spectral range [2].

tissue is therefore nonlinear and confined to the focal volume. The nonlinear nature of the interaction makes it possible to apply femtosecond imaging and dissection to any transparent material. A second advantage is that at a pulse duration of about 100 fs, only a few nanojoules of energy are necessary for material dissection [6,10]. In contrast, cutting with green picosecond laser systems [11,12] and UV laser microscissors [13,14] requires energies that are two to three orders of magnitude higher [15]. The low energy of the femtosecond laser pulses minimizes the size of the cavitation bubbles created by the deposited energy and limits the dissection width to several hundred nanometers. The low energy also causes negligible collateral damage around the laser focus, reducing the likelihood that the cell will be injured or killed.

The use of femtosecond lasers for nanoprocessing of subcellular structures has steadily increased since 1995, when König et al. [7] demonstrated the dissection of isolated human chromosomes. The width of femtosecond laser cuts was measured using atomic force microscopy and fluorescence microscopy [7]. The same group created a small puncture in the cell membrane and infused DNA in the cell, with 100% expression efficiency and cell survival rate [8]. Other work includes the ablation in *Drosophila* embryos [16] and the photodisruption of single mitochondria [9]. Femtosecond pulses were also successfully used in place of mechanical microkeratomes in the cornea incision in corrective eye surgery, leading to smaller wound healing reaction [17,18]. Neurons in live *C. elegans* show photobleaching when irradiated by highly focused femtosecond pulses (1.4 NA) at pulse energies of 1–2 nJ, and much higher energies of 10–40 nJ were used to sever the neurons [19].

Femtosecond lasers are a useful tool for the imaging and study of biological structures and processes with a submicrometer spatial resolution. They can be used to dissect isolated structures, perform subcellular nanosurgery of individual organelles and disrupt cells within living animals. In this paper we review work done in our group on the pulse energy dependence of femtosecond laser ablation in fluorescently-labeled structures in the cytoskeleton and nuclei of fixed cells using a combination of fluorescence microscopy and transmission electron microscopy (TEM). We also present a series of nanosurgery experiments performed on subcellular structures in live cells and we show the dissection of a single neuron within a dense neural bundle in *C. elegans*.

Experimental methods

The experiments presented here were carried out using a custom-built fluorescence microscope integrated with a femtosecond laser system (Fig. 2a). The Ti:sapphire laser is a home-built system consisting of an oscillator and a chirped-pulse amplification system. The passively mode-locked oscillator delivers 100-fs pulses at a repetition rate of 80 MHz and a central wavelength of 800 nm. These pulses are regeneratively amplified to energies of 0.5 mJ at a repetition rate of 1 kHz. These energies are far too high for subcellular ablation and are attenuated to the nanojoule range. The laser light is focused into the sample with a 1.4-NA oil-immersion objective (Zeiss, Plan-Apochromat), yielding a theoretical spot size of 340 nm. Because of group-velocity dispersion inside the microscope objective, the laser pulses are stretched to 200–250 fs at the sample [2]. The sample is placed on a piezo-controlled microscope stage that permits sample positioning with 10-nm precision along all three axes. A mercury-arc lamp illuminates the sample and the emitted fluorescence is collected through the objective using a standard filter cube and imaged in real time with a CCD camera.

Recently we upgraded the system, combining laser nanosurgery with simultaneous high-resolution, scanning multiphoton imaging as shown in Fig. 2b. Half the train from a 80-MHz, 60-fs oscillator is used in a custom-built two-photon microscope [20] and used for imaging. The other half of the pulse is amplified by a regenerative amplifier, yielding a 250-kHz pulse train of 60-fs duration and 4-μJ pulse energy. This beam is attenuated to 2–5 nJ per pulse and then used for dissection.

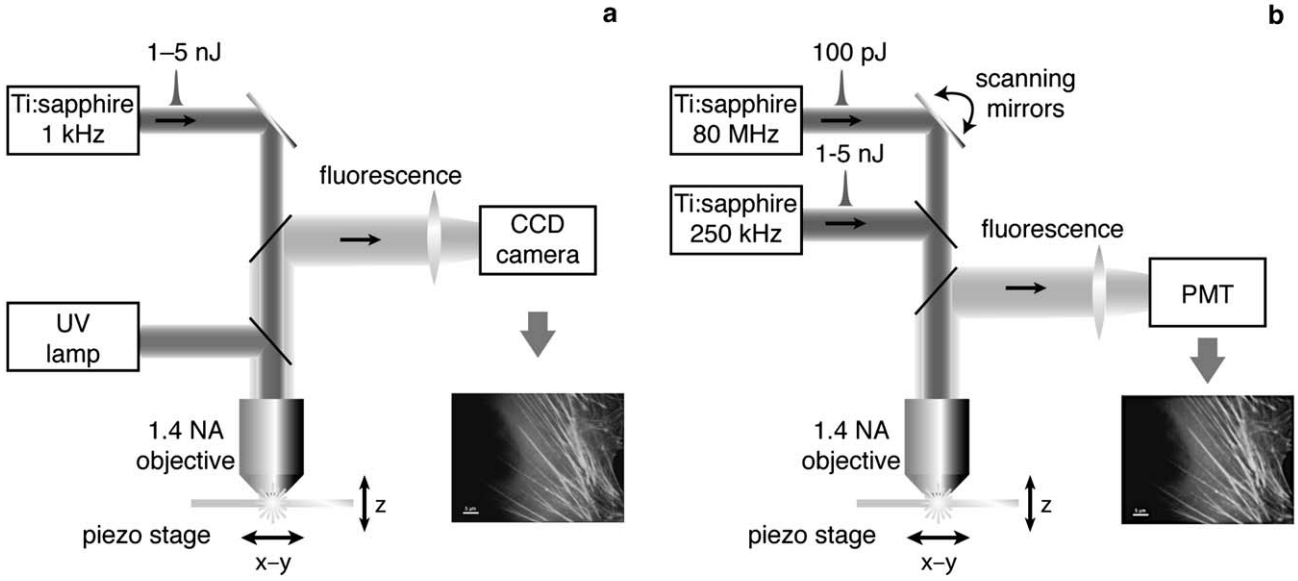

Fig. 2. Schematic diagrams of experimental setups for nanosurgery. A dissecting laser beam can be combined with (a) a fluorescence microscope or (b) a two-photon microscope.

Results and discussion

To demonstrate the capabilities of the nanosurgical technique, we first used the femtosecond laser to ablate the actin cytoskeleton within bovine endothelial cells that were stained with the green fluorescent F-actin-binding dye, Alexa Fluor 488-phalloidin [6]. Fig. 3a shows the fluorescence from a fixed endothelial cell after irradiation with various pulse energies along five parallel lines. The nanometer scale channels within the cytoskeleton were obtained by translating the cell at 0.7 μm/s in a direction perpendicular to the laser beam. Fig. 3b shows that the fluorescence intensity following irradiation depends strongly on pulse energy. At 1.8 nJ the effect of irradiation is barely visible in the fluorescence image. Increasing the pulse energy to 2.2 nJ produces a clear dip in fluorescence with a full-width at half-maximum (FWHM) of 240 nm. At higher energy, the FWHM width of the dip in fluorescence scales with pulse energy, from 360 nm at 2.8 nJ, to 500 nm at 3.5 nJ and 600 nm at 4.4 nJ.

The fluorescence signal from samples is widely used in biological imaging, and thus it would be convenient to use it also to determine the laser-mediated dissection width. For example, one might want to use the lowest feasible energy to achieve the narrowest cuts and the least damage outside the focal volume. However, near threshold it is not clear whether the decrease in fluorescence is due to photobleaching or material removal. To determine the thresholds for laser-induced photobleaching and material removal, we compared fluorescence images of laser-irradiated cells to TEM images. The TEM analysis gives a direct measure of the ablated area, as the electrons are sensitive to the amount of material they travel through. The ablated region appears lighter on the film, even if it is confined in the bulk of the sample.

Fig. 4 shows that loss of fluorescence does not always correspond to removal of material. The figure shows both fluorescence and TEM images of the nucleus of the same fixed endothelial cell after irradiation at three different energies. While a slight loss of fluorescence can be observed for a pulse energy of 1.45 nJ, the TEM image shows no material removal at that pulse energy. Thus, the observed loss of fluorescence at 1.45 nJ must be due to photobleaching. At higher energies there is clear ablation in both images.

The comparison of the fluorescence and the TEM images allows us to define three regimes of irradiation: no interaction (no damage visible in either image), photobleaching without material loss (only the fluorescence image shows a change), and removal of material (both images show changes). While the absolute energy threshold varies somewhat from sample to sample, the data consistently show that the threshold for plasma-mediated ablation is never more than 20% higher than that for photobleaching. Therefore, fluorescence microscopy can be used to confirm dissection, as long as the energy exceeds 1.2 times the threshold for photobleaching.

The TEM and fluorescence microscopy measurements also reveal that the plasma-mediated ablation width strongly depends on pulse energy. Pulse energies between 1.2 and 1.7 nJ produce cuts as narrow as 200 nm. Above 1.7 nJ, the dissection width increases with energy; around 3 nJ the width is approximately 1 μm.

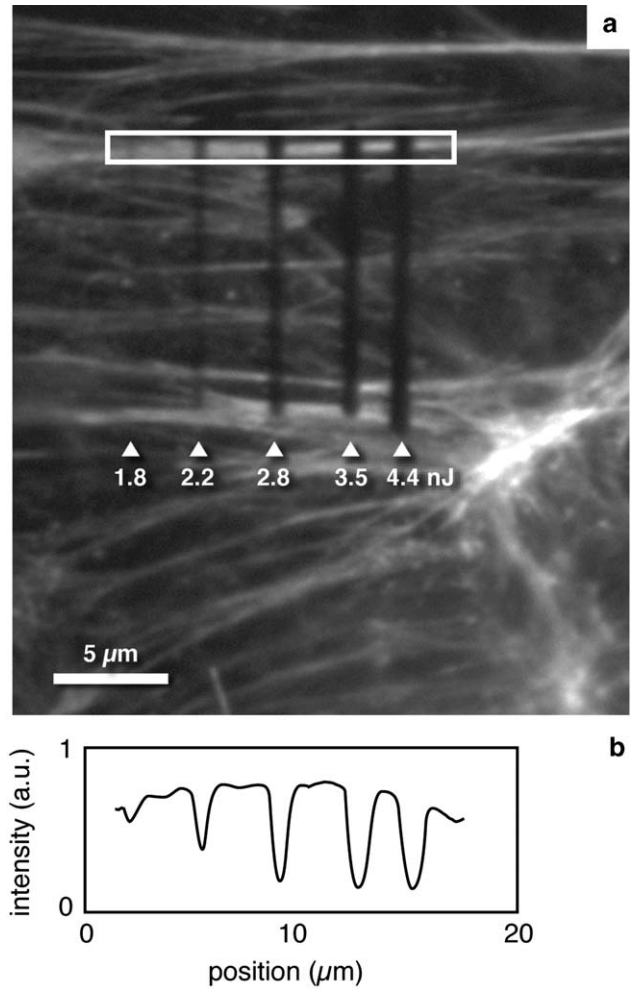

Fig. 3. (a) Cuts through fluorescently-labeled actin fibers in a fixed endothelial cell obtained by irradiation with femtosecond laser pulses of energies between 1.8 and 4.4 nJ. (b) Fluorescence intensity profile along the actin bundle outlined in the image.

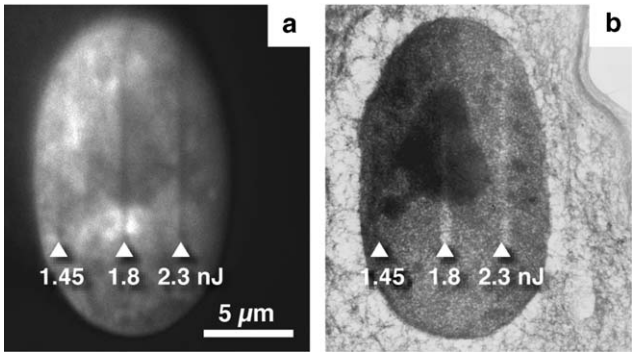

Fig. 4. Cuts in the nucleus of a fixed endothelial cell at various laser energies, imaged by (a) fluorescence microscopy and (b) electron microscopy.

The fixed cell experiments allowed us to establish the feasibility of the nanosurgery technique and determine the optimal energy range. We applied the technique to study the organization of mitochondria on the nanometer scale in endothelial cells [5]. Some studies suggest that these energy-generating organelles form a physically continuous network similar to the endoplasmic reticulum [21,22], while others suggest that mitochondria are organized as structurally independent functional units [23,24] that are linked by cytoskeletal filaments [25,26]. We probed the connectivity of the mitochondria by damaging a single mitochondrion and observing the effects on its neighbors.

To visualize the mitochondria, capillary endothelial cells were transfected with Enhanced Yellow Fluorescent Protein (EYFP) fused to cytochrome C oxidase [25,27] (Fig. 5a), and the sample was positioned such that the laser was focused in the middle of a single mitochondrion. Figs. 5b and c show the ablation of a single mitochondrion, about 5 μm in length and separated by less than 1 μm from multiple neighboring mitochondria. After irradiating a fixed spot on the organelle with a few hundred 2-nJ laser pulses at a 1-kHz repetition rate, the entire mitochondrion disappears from the image, whereas neighboring mitochondria are not affected by the irradiation despite being only a few hundred nanometers away (Fig. 5c). Even though the laser is focused to a 0.5-μm diameter spot in the center of the mitochondrion and remains stationary during the irradiation time, the fluorescence immediately disappears throughout the entire mitochondrion over a length scale of up to tens of micrometers. These observations demonstrate that local ablation causes a major structural change in the target mitochondrion and results in destruction of the entire mitochondrion, but not its neighbors. This result provides clear evidence that mitochondria do not form a structurally continuous network as previously suggested [21,22].

While the dissection of a single mitochondrion did not cause any apparent distress to the cell, we performed a test to verify that the membrane is not ruptured during the nanosurgery [5]. To this end we carried out similar

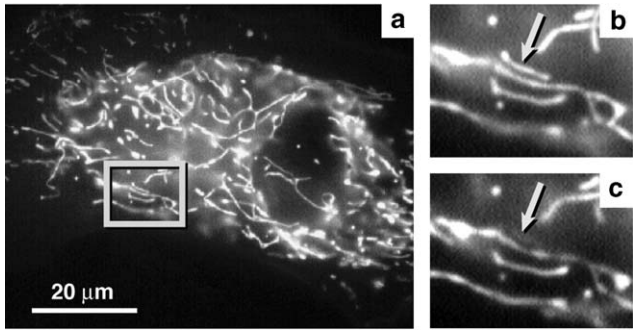

Fig. 5. Ablation of a single mitochondrion in a living cell: (a) fluorescence microscope image showing multiple mitochondria before femtosecond laser irradiation. Target mitochondrion (marked by arrow) (b) before and (c) after laser ablation with 2-nJ pulses.

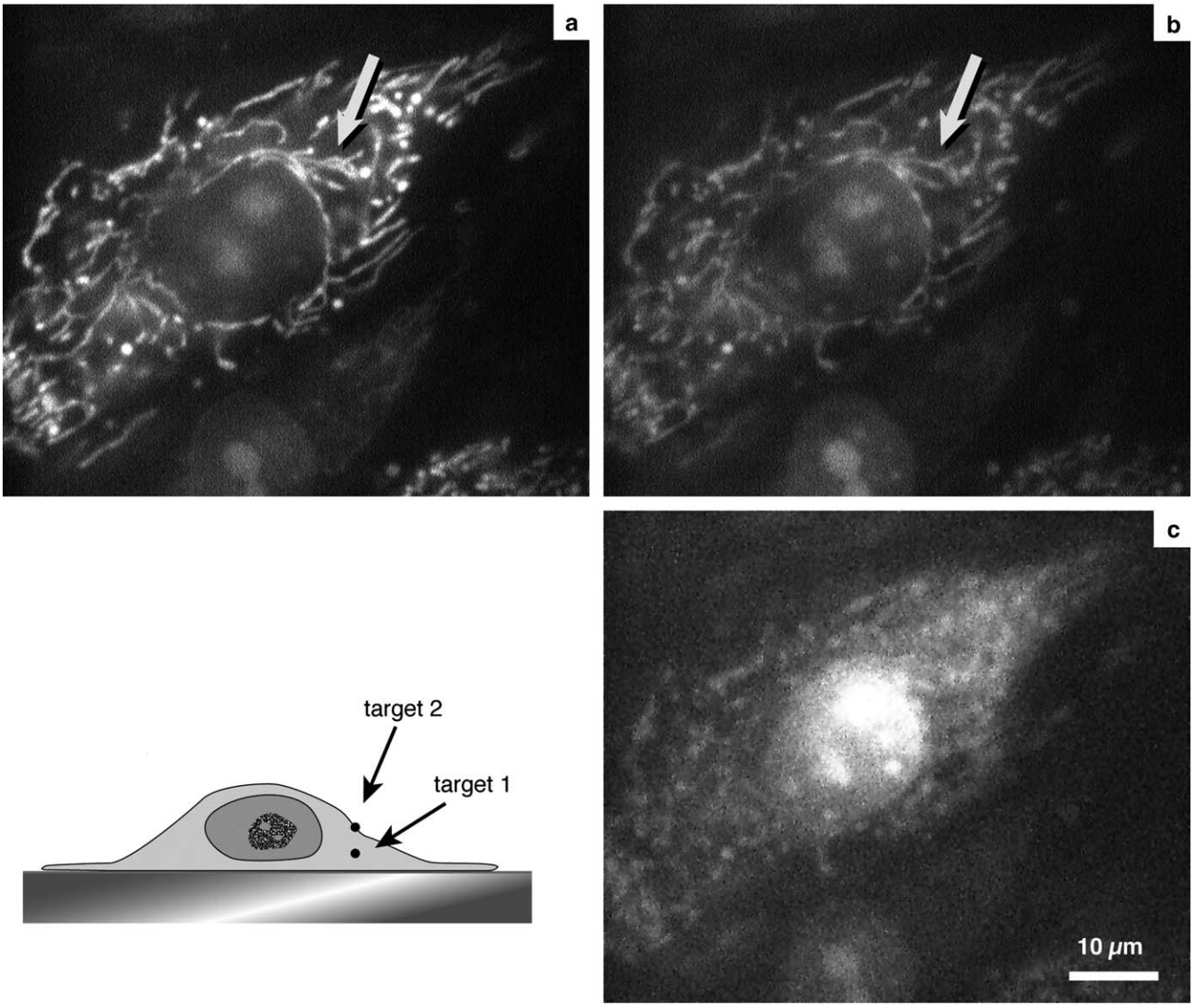

Fig. 6. Ablation of a mitochondrion in a live cell without compromising cell viability. Fluorescence microscope images of a live cell containing EYFP-labeled mitochondria in a cultured medium containing ethidium bromide (a) before femtosecond laser irradiation, (b) after ablation of a single mitochondrion within its cytoplasm (target 1 in diagram at bottom left), and (c) after irradiation of the apical cell membrane (target 2). An increase in nuclear ethidium bromide staining is only observed after irradiation of the apical membrane.

experiments in cells that were incubated with the DNA-binding dye ethidium bromide. The dye cannot penetrate through the cell membrane and little nuclear fluorescence is observed in living cells prior to laser exposure (Fig. 6a). After dissecting a single mitochondrion with 2-nJ pulse energy we did not detect any change in the nuclear fluorescence (Fig. 6b). In contrast, when we focused the laser beam at the top surface of the cell and irradiated the apical cell membrane, the intensity of fluorescent signal from the nucleus immediately increased by a factor of ten as the ethidium bromide rapidly diffused into the cell through the incision in the surface membrane (Fig. 6c). In conjunction with the absence of any morphological changes in the cell or other mitochondria over a period of 1 h following ablation, these results show that nanosurgery can be used to selectively ablate internal cell structures without inflicting generalized injury or causing cell necrosis.

To further test the precision of our nanosurgery system and its application to various subcellular structures we turned our attention to the microtubule network [6]. The microtubule network is sensitive to external disruptions and can be used as a good indicator for the extent of damage induced by laser irradiation outside the focal volume. Fig. 7a shows a fluorescence

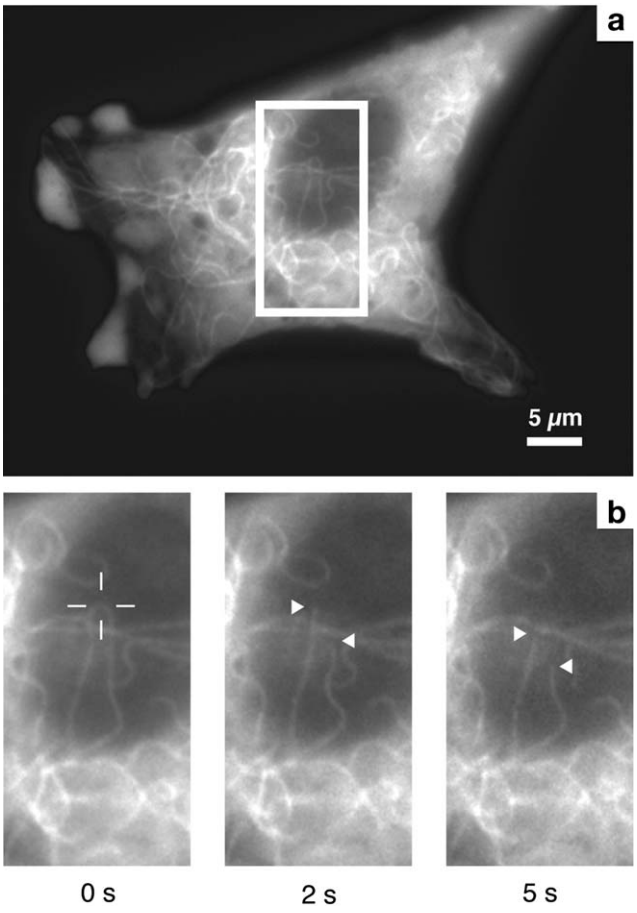

Fig. 7. (a) Fluorescence microscope image of GFP-labeled the microtubule network in an endothelial cell. (b) Time-lapse sequence showing rapid retraction of microtubule due to elastic retraction followed by depolymerization. The cross hairs indicate the area targeted by the laser; the triangles show the retracting ends of the microtubule.

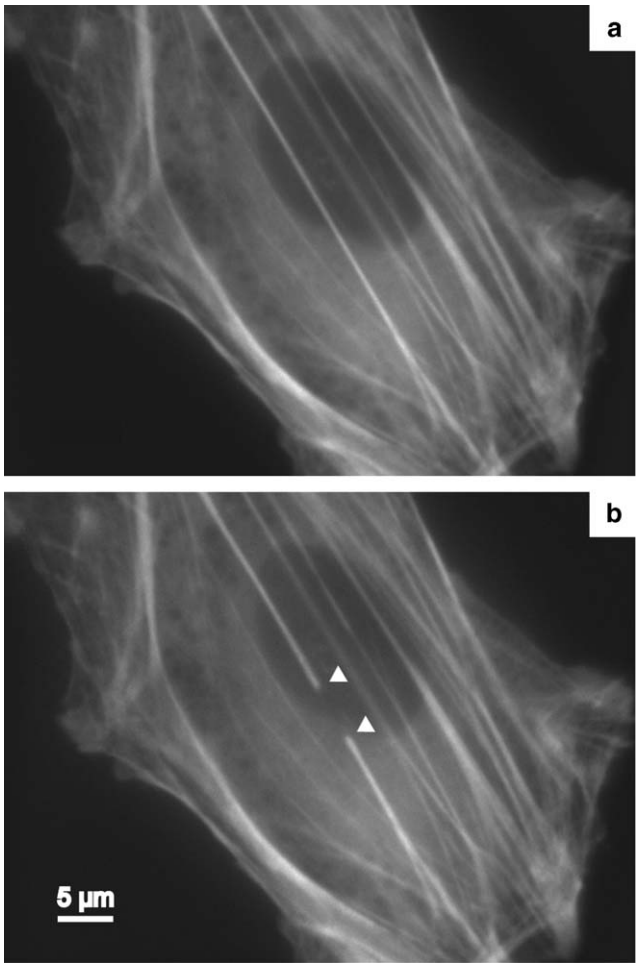

Fig. 8. Fluorescence microscope images of the YFP-labeled actin network in an endothelial cell (a) before and (b) 4 s after laser dissection of an actin fiber bundle. The triangles show the retracting ends of the bundle.

microscope image of a live bovine endothelial cell which was transfected with an adenoviral vector system [28,29] encoding enhanced green fluorescent protein tagged G-tubulin. The dark region in the middle of the cell is the nucleus. We severed a bent region of a single microtubule right over the nucleus using about 1000 laser pulses with a pulse energy of 1.5 nJ. The curved end of the microtubule immediately recoiled, returning to a straight configuration within the first 2 s after laser ablation. The immediate recoil indicates the release of stored elastic energy in the molecular filament. The time-lapse frames in Fig. 7b show that the initial recoil is followed by depolymerization of the cut ends of microtubule due to release of tubulin monomers. Neighboring microtubules, which are less than 1 μm away, remain undisturbed.

We also studied the actin filaments of endothelial cells, which form the underlying stress fiber network in the cells. Many measurements of the properties of actin networks have been carried out in vitro, but there has been no direct physical probe of single stress fibers in their natural cellular environment. We visualized the actin stress fibers by transfecting the endothelial cells with YFP-tagged G-actin. We targeted the laser light onto a single fiber and irradiated it with a few hundred laser pulses. Fig. 8 shows a fluorescence image of the actin network before and four seconds after irradiation. After dissection of the actin fiber the distance between the severed ends grows to many times that of the 0.5-μm-diameter laser focus, showing the response of the cell to the mechanical disruption of the stress fiber.

In addition to probing subcellular structure, femtosecond lasers can be used to dissect cells within living tissues or animals. The nematode worm, *C. elegans*, is particularly well suited for femtosecond laser dissection due to its transparency and size. While the low spatial selectivity of conventional laser systems limited previous surgeries to larval-stage ablation of whole cell bodies

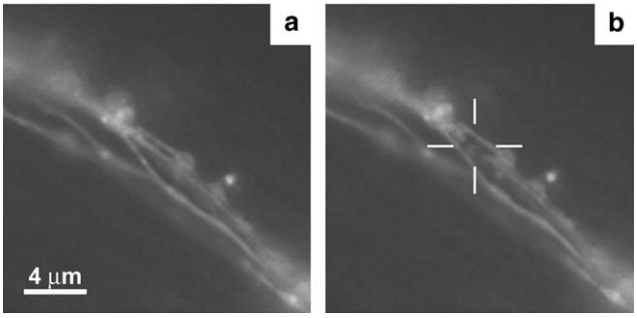

Fig. 9. Amphid neuron bundle in *C. elegans* (a) before and (b) after dissection with 3.6-nJ pulses. The cross hairs indicate the area targeted by the laser. The center dendrite is severed while the outer two are undamaged.

[30], femtosecond lasers permit dissection of much smaller structures in adult worms. Thus, we circumvent issues arising from post-surgery development, which is not well understood. Fig. 9 shows a bundle of fluorescently labeled neurons where the middle neuron was severed without disruption of the neighboring neurons.

The invariant neural circuit of *C. elegans* totals 302 neurons and encodes a universal behavior, and the study of the individual neuron function has been limited to observing behavioral changes in mutant worms. Femtosecond laser dissection enables us to directly observe the function of individual neurons by severing neuronal fibers, much like cutting wires in an electrical circuit. The function of a neuron or neuronal part can then be identified by observing behavioral changes after the surgery.

Conclusion

In this review, we have summarized recent progress in determining the precision and spatial selectivity of femtosecond laser dissection and developing applications for subcellular nanoprocessing. We determined the relationship between pulse energy and material loss after femtosecond laser irradiation. The optimal energy range for plasma-mediated ablation is from about 20% above the photobleaching threshold to about 3 nJ. In this range we can dissect biological samples with a resolution of 200 nm. We also demonstrated that this technique could be applied to live cells to probe relevant biological questions that require high spatial discrimination. We have shown that the mitochondria are individual organelles that are not part of an interconnected network and we probed the cytoskeletal mechanics by severing single microtubules and actin stress fibers.

The use of ultrashort laser pulses for dissecting and imaging cells and subcellular structures in cellular and developmental biology is increasing rapidly. Recent improvements in laser technology and the commercial availability of multiphoton microscopes allow this technique to be used in labs that do not specialize in femtosecond optics. Other commercial medical applications of femtosecond laser systems exist in eye surgery and in high-precision laser-based microtomes for three-dimensional tissue and material cutting. However, there are still open questions about the exact mechanism of the plasma-mediated ablation, thermal effects due to energy accumulation in high-repetition rate laser irradiation, and pulse-to-pulse interactions.

Acknowledgements

The authors would like to thank the many people who have contributed to this work over the years: Nozomi Nishimura, Chris Schaffer, Nan Shen, Debajyoti Datta, Philip LeDuc, Jean Underwood, Jeffrey Nickerson, Sanjay Kumar, Alexander Heisterkamp, Aravinthan Samuel and Donald Ingber. This work was supported by the National Science Foundation under Grant DMR-0213805.

Zusammenfassung

Nano-Manipulation von subzellularen Strukturen mit dem Femtosekundenlaser

In diesem Artikel stellen wir unsere Arbeiten zur Zellchirurgie mit dem Femtosekundenlaser in einzelnen Zellen und lebenden Organismen vor. Gezieltes Manipulieren von biologischen Materialien mittels ultrakurzer Laserpulse erfordert ein tiefergehendes Verständnis, inwieweit die Schwelle zur Plasmazündung und Umfang der plasma-induzierten Ablation (d.h. der Abtrag von Gewebe) von der Pulsenergie abhängen. In diesem Zusammenhang führten wir eine systematische Studie bzgl. der Schwellenergie zur Plasmaerzeugung bei fester Fokussierung in fluoreszenz-markierten subzellulären Strukturen wie Cytoskelett und Zellkern in fixierten Rinderendothelzellen mittels nahinfraroter Femtosekunden Laserpulse durch. Die Laserpulse wurden über ein Mikroskopobjektiv mit hoher numerischer Apertur (NA = 1,4) fokussiert. Im weiteren Verlauf konnten wir diese Laser-Nanochirurgie in lebenden Zellen umsetzen und so einzelne Mitochondrien entfernen und einzelne Bestandteile des Cytoskeletts durchtrennen, ohne die Zellmembran oder die Zellintegrität zu beeinträchtigen. Mittels dieser Technik gelang es uns auch, einzelne Dendriten in lebenden *C. elegans* Nematoden zu durchschneiden, ohne direkt benachbarte Nervenzellen zu beschädigen. Die vorgestellte Nano-Manipulationstechnik ermöglicht eine nicht-invasive Handhabung einzelner Bestandteile der inneren Maschinerie von

Zellen und Gewebe, verbunden mit Auflösungen bis in den Bereich weniger hundert Nanometer.

Schlüsselwörter: Femtosekundenlaser; Nanochirurgie

References

[1] Denk W, Strickler JH, Webb WW. Two-photon laser scanning fluorescence microscopy. Science 1990;248:73–6.
[2] Koenig K. Multiphoton microscopy in life sciences. J Microsc 2000;200:83–104.
[3] Stern D, Schoenlein RW, Puliafito CA, Dobi ET, Birngruber R, Fujimoto JG. Ablation by nanosecond, picosecond, and femtosecond lasers at 532 nm and 625 nm. Arch Ophthalmol 1989;107:587–92.
[4] So PTC, Kim H, Kochevar IE. Two-photon deep tissue ex vivo imaging of mouse dermal and subcutaneous structures. Opt Express 1998;3:339–50.
[5] Shen N, Datta D, Schaffer CB, Le Duc P, Ingber DE, Mazur E. Ablation of cytoskeletal filaments and mitochondria in live cells using a femtosecond laser microscissors. Mech Chem Biosyst 2005;2:17–26.
[6] Heisterkamp A, Maxwell IZ, Mazur E, Underwood JM, Nickerson JA, Kumar S, et al. Pulse energy dependence of subcellular dissection by femtosecond laser pulses. Opt Express 2005;13:3690–6.
[7] Koenig K, Riemann I, Fischer P, Halbhuber K. Intracellular nanosurgery with near infrared femtosecond laser pulses. Cell. Mol. Biol. 1995;45:192–201.
[8] Tirlapur UK, Koenig K. Targeted transfection by femtosecond laser. Nature 2002;448:290–1.
[9] Watanabe W, Arakawa N, Matsunaga S, Higashi T, Fukui K, Isobe K, et al. Femtosecond laser disruption of subcellular organelles in a living cell. Opt Express 2004;12:4203–13.
[10] Vogel A, Venugopalan V. Mechanisms of pulsed laser ablation of biological tissues. Chem Rev 2003;103:577–644.
[11] Berns MW, Aist J, Edwards J, Strahs K, Girton J, McNeil P, et al. Laser microsurgery in cell and developmental biology. Science 1981;213:505–13.
[12] Liang H, Wright WH, Cheng S, He W, Berns MW. Micromanipulation of chromosomes in PTK2 cells using laser microsurgery (optical scalpel) in combination with laser-induced optical force (optical tweezers). Exp Cell Res 1993;204:110–20.
[13] Aist JR, Liang H, Berns MW. Astral and spindle forces in PTK2 cells during anaphase B: a laser microbeam study. J Cell Sci 1993;104:1207–16.
[14] Grill SW, Howard J, Schäffer E, Stelzer EHK, Hyman AA. The distribution of active force generators controls mitotic spindle position. Science 2003;301:518–21.
[15] Noack J, Hammer DX, Noojin GD, Rockwell BA, Vogel A. Influence of pulse duration on mechanical effects after laser-induced breakdown in water. J Appl Phys 1998;83:7488–95.
[16] Supatto W, Debarre D, Moulia B, Brouzes E, Martin J, Farge E, et al. In vivo modulation of morphogenetic movements in *Drosophila* embryos with femtosecond laser pulses. Proc Natl Acad Sci USA 2005;102:1047–52.
[17] Juhasz T, Djotyan G, Loesel FH, Kurtz RM, Horvath C, Bille JF. Laser Phys 2000;10:495–500.
[18] Heisterkamp A, Ripken T, Mamom T, Drommer W, Welling H, Ertmer W, et al. Nonlinear side effects of fs pulses inside corneal tissue during photodisruption. Appl Phys B 2002;74:1–7.
[19] Yanik MF, Cinar H, Cinar HN, Chisholm AD, Jin Y, Ben-Yakar A. Neurosurgery: functional regeneration after laser axotomy. Nature 2004;432:822.
[20] Tsai PS, Nishimura N, Yoder EJ, White A, Dolnick E, Kleinfeld D. Principles, design and construction of a two photon scanning microscope for in vitro and in vivo studies. In: Frostig R, editor. Methods for in vivo optical imaging. Boca Ration: CRC Press; 2002. p. 113–71.
[21] De Giorgi F, Lartigue L, Ichas F. Electrical coupling and plasticity of the mitochondrial network. Cell Calcium 2000;28:365–70.
[22] Rizzuto R, Pinton P, Carrington W, Fay FS, Fogarty KE, Lifshitz LM, et al. Close contacts with the endoplasmic reticulum as determinants of mitochondrial Ca+ responses. Science 1998;280:1763.
[23] Park MK, Ashby MC, Erdemli G, Petersen OH, Tepikin AV. Perinuclear, perigranular and sub-plasmalemmal mitochondria have distinct functions in the regulation of cellular calcium transport. EMBO J 2001;20:1863–74.
[24] Collins TJ, Berridge MJ, Lipp P, Bootman MD. Mitochondria are morphologically and functionally heterogeneous within cells. EMBO J 2002;21:1616–27.
[25] Wang N, Naruse K, Stamenovic D, Fredberg JJ, Mijailovich SM, Tolic- Norrelykke IM, et al. Mechanical behavior in living cells consistent with the tensegrity model. Proc Natl Acad Sci USA 2001;98:7765–70.
[26] Lin A, Krockmalnic G, Penman S. Imaging cytoskeleton-mitochondrial membrane attachments by embedment-free electron microscopy of spaonin-extracted cells. Proc Natl Acad Sci USA 1990;87:8565–9.
[27] Huang Z, Tamura M, Sakurai T, Chuma S, Saito T, Kakatsuji M. In vivo transfection of testicular germ cells and transgenesis by using the mitochondrially localized jellyfish fluorescent protein. FEBS Lett 2000;487:248–51.
[28] Numaguchi Y, Huang S, Polte TR, Eichler GS, Wang N, Ingber DE. Caldesmon-dependent switching between capillary endothelial cell growth and apoptosis through modulation of cell shape and contractility. Angiogenesis 2003;6:55–64.
[29] Hu SH, Chen JX, Wang N. Cell spreading controls balance of prestress by microtubules and extracellular matrix. Front Biosci 2004;9:2177–82.
[30] Bargmann CI, Avery L. Laser killing of cells in *Caenorhabditis elegans*. Methods Cell Biol 1995;48:225–50.